Boundary symmetry breaking of flocking systems

Leonardo Lenzini,[1,2] Giuseppe Fava,[1,2] and Francesco Ginelli[1,2]

[1] *Dipartimento di Scienza e Alta Tecnologia, Università degli Studi dell'Insubria and Center for Nonlinear and Complex Systems, via Valleggio 11, 22100, Como, Italy*
[2] *INFN Sezione di Milano, 20133, Milano, Italy*

We consider a flocking system confined transversally between two infinite reflecting parallel walls separated by a distance $L_\perp$. Infinite or periodic boundary conditions are assumed longitudinally to the direction of collective motion, defining a ring geometry typical of experimental realizations with flocking active colloids. Such a confinement selects a flocking state with its mean direction aligned parallel to the wall, thus breaking explicitly the rotational symmetry locally by a boundary effect. Finite size scaling analysis and numerical simulations show that confinement induces an effective mass term $M_c \sim L_\perp^{-\zeta}$ (with positive ζ being equal to the dynamical scaling exponent of the free theory) suppressing scale free correlations at small wave-numbers. However, due to the finite system size in the transversal direction, this effect can only be detected for large enough longitudinal system sizes (i.e. narrow ring geometries). Furthermore, in the longitudinal direction, density correlations are characterized by an anomalous effective mass term. The effective mass term also enhances the global scalar order parameter and suppresses fluctuations of the mean flocking direction. These results suggest an equivalence between transversal confinement and driving by an homogeneous external field, which breaks the rotational symmetry at the global level.

I. INTRODUCTION

It is well known that locally aligning self-propelled particles may achieve global polar order and move collectively in a state known as *flocking* [1, 2], a collective phenomenon observed in systems as diverse as bird flocks [3], cellular migration [4], motility assays [5] or active colloids[6]. When polar order emerges in an isotropic environment, it does so by spontaneously breaking the underlying continuous rotational symmetry, a fact that largely determines the large scale physics of flocking systems [7]. While the non-equilibrium nature of active matter systems allows flocks to escape the constraints of the Mermin-Wagner-Hohenberg theorem [8, 9] and achieve long-range order even in two spatial dimensions [10], the symmetry-broken phase is nevertheless characterized by massless modes (the *Nambu-Goldstone modes*) and consequently by long-range correlations. Notably, long-ranged (or scale-free) correlations have been measured both in starling flocks [11] and in *in vitro* cellular migration [4]: despite the innumerable differences between these systems and minimal self-propelled particles models, their large-scale behavior is determined by simple symmetry considerations.

The large-scale, long time behavior of flocks is described by the seminal Toner & Tu (TT) fluctuating hydrodynamic theory [10, 12, 13]. While the exact value of the TT scaling exponents has long remained elusive, recent large-scale simulations [14] and analytical breakthrough [15, 16] seem to have settled the issue.

Flocking, however, may also take place in anisotropic environments, where the rotational symmetry is explicitly broken. Cell motility, for instance, is known to be sensitive to a wide range of external gradients of chemical (chemotaxis), mechanical (durotaxis), and electrical (electrotaxis) origin which often direct cellular migrations. The response of flocking systems to a global, homogeneous external field $\mathbf{h}$ leading the direction of motion of individual particles has been discussed in the linear regime by Refs. [17, 18]. In particular, it is easy to show that the external field generates an effective mass term and an exponential cut off of fluctuation correlations.

In this work, on the other hand, we want to investigate flocking in the presence of an explicit symmetry breaking at the system boundaries. This is relevant for many experimental realisations with active colloids, where confinement by hard boundaries (e.g., within a ring [6]) is practically unavoidable. Specifically, we consider a d dimensional flocking system confined in an infinite channel of width $L_\perp$ by reflecting boundaries conditions in $d-1$ *transversal* spatial directions. Such a confinement explicitly breaks rotational invariance at the boundaries, selecting a preferred direction along the free direction (hereafter denoted as the *longitudinal* direction) and effectively forcing collective motion along the channel. In finite systems, one can assume periodic boundary conditions along the free directions, obtaining a ring geometry as in certain active colloids experimental realisations [19]. This setup has been also employed in numerical investigations of flocking models [14, 20] as a way to suppress the diffusion of the mean flock orientation in finite systems. The underlying assumption of these numerical studies is that fluctuations correlations measured in the bulk (that is, sufficiently far away from the reflecting boundaries) are left unperturbed by the boundary symmetry breaking.

In this work we verify explicitly these assumptions. While finite size scaling analysis reveals that transversal confinement induces an effective mass term – damping transversal fluctuations and potentially cutting off correlations above a certain length scale – it can also be shown that this exponential cut-off cannot be detected in typical (and finite) confined geometries, effectively validating

the assumption of unperturbed bulk correlations. Interestingly, this behavior is formally equivalent to that of a flocking system perturbed (in the linear regime) by an homogeneous external field of amplitude h, provided that

$$h \sim L_{\perp}^{-z} \tag{1}$$

where z is the dynamical scaling exponent of TT theory. This equivalence extends to other static properties such as the response and the fluctuations of the global polar order parameter.

II. STATIC CORRELATION FUNCTIONS

A. Brief review of bulk theory

We first discuss the effect of confinement on the correlation functions of the relevant slow hydrodynamic fields. In order to do so, we first briefly review the TT equations [10, 13] which rule the slow, long-wavelength dynamics of the conserved density $\rho(\mathbf{r},t)$ and velocity $\mathbf{v}(\mathbf{r},t)$ fields,

$$\partial_t \rho + \nabla\cdot(\rho\mathbf{v}) = 0\,, \tag{2}$$

$$\begin{aligned}\partial_t\mathbf{v} + \lambda_1(\mathbf{v}\cdot\nabla)\mathbf{v} + \lambda_2(\nabla\cdot\mathbf{v})\mathbf{v} + \lambda_3\nabla|\mathbf{v}|^2 \\ =(\alpha-\beta|\mathbf{v}|^2)\mathbf{v} - \nabla P_1 - \mathbf{v}(\mathbf{v}\cdot\nabla P_2) + D_1\nabla(\nabla\cdot\mathbf{v}) \\ + D_3\nabla^2\mathbf{v} + D_2(\mathbf{v}\cdot\nabla)^2\mathbf{v} + \mathbf{f}.\end{aligned} \tag{3}$$

Here all the phenomenological convective (λ_i, with $i = 1,2,3$) and viscous ($D_i > 0$) coefficients, as well as the two symmetry breaking ones, α and β, can in principle, depend on ρ and $|\mathbf{v}|$ and the pressures $P_{1,2}$ may be expressed as a series in the density. The additive noise term $\mathbf{f}$ has zero mean, variance Δ and is delta correlated in space and time. For $\alpha > 0$, these equations can be linearized around the homogeneous stationary ordered solution of the fluctuation-less dynamics, $\rho(\mathbf{r}) = \rho_0 + \delta\rho(\mathbf{r})$ and $\mathbf{v}(\mathbf{r}) = (p_0 + \delta v_{\parallel}(\mathbf{r}))\hat{\mathbf{e}}_{\parallel} + \mathbf{v}_{\perp}(\mathbf{r})$, with $\hat{\mathbf{e}}_{\parallel}$ being the unit vector along the direction of collective motion and $p_0 = \sqrt{\alpha_0/\beta_0}$ [1]. Here and in the following the subscripts $\parallel$ and $\perp$ denote, respectively, the longitudinal and transversal vector components w.r.t. the reflecting boundaries. Once the fast longitudinal field $\delta v_{\parallel}(\mathbf{r})$ is enslaved away

$$\delta v_{\parallel} \approx -\frac{|\mathbf{v}_{\perp}|^2}{2p_0} - \frac{\Gamma_2}{\Gamma_1}\left(\delta\rho - \frac{\partial_t\delta\rho}{p_0\Gamma_1} + \frac{\lambda_4\partial_{||}\delta\rho}{\Gamma_2}\right) - \frac{\lambda_2}{\Gamma_1}\nabla_{\perp}\cdot\mathbf{v}_{\perp} \tag{4}$$

(see Ref. [13] for more details and the definition of the here unimportant coefficients λ_4, Γ_1 and Γ_2), one is left with two linear equations for the slow hydrodynamic fields $\delta\rho(\mathbf{r})$ and $\mathbf{v}_{\perp}$ – the velocity field transversal to $\hat{\mathbf{e}}_{\parallel}$ – that can be readily solved.

Here we focus on the equal time Fourier space fluctuations correlations (or *structure factors*) that for small wave-numbers $q = |\mathbf{q}|$ read

$$S_{\rho}(\mathbf{q},\boldsymbol{\mu}^{(1)}) \equiv \langle|\delta\hat{\rho}(\mathbf{q})|^2\rangle \sim A(\theta_{\mathbf{q}},\boldsymbol{\mu}^{(1)})\,q^{-2} \tag{5}$$

and

$$S_{v}(\mathbf{q},\boldsymbol{\mu}^{(1)}) \equiv \langle|\hat{v}_{\perp}(\mathbf{q})|^2\rangle \sim B(\theta_{\mathbf{q}},\boldsymbol{\mu}^{(1)})\,q^{-2}\,, \tag{6}$$

where $\langle\cdot\rangle$ denotes ensemble averages and $A(\theta_{\mathbf{q}},\boldsymbol{\mu}^{(1)})$ and $B(\theta_{\mathbf{q}},\boldsymbol{\mu}^{(1)})$ depend on the TT equation coefficients, here collectively denoted as $\boldsymbol{\mu}^{(1)}$, and on the angle $\theta_{\mathbf{q}}$ between $\mathbf{q}$ and $\hat{\mathbf{e}}_{\parallel}$. It is convenient to introduce the longitudinal and transversal components of the wave-vector, $\mathbf{q} = (\mathbf{q}_{\perp}, q_{\parallel})$, so that $q_{\parallel} = q\cos\theta_{\mathbf{q}}$ and $q_{\perp} \equiv |\mathbf{q}_{\perp}| = \sin\theta_{\mathbf{q}}$. The precise expression for A and B is irrelevant for the following and can be found in Ref. [13], but it should be noted that the amplitude A is singular in the longitudinal direction, $A(0,\boldsymbol{\mu}^{(1)}) = 0$, so that the linear behavior of S_{ρ} for $q_{\perp}\to 0$ cannot be determined at this order in TT theory.

Nonlinearities, moreover, turn out to be relevant in $d < d_c = 4$. *Inter alia*, this is what prevents the linearized fluctuations (6) to destroy long-range order due to their non-integrable divergence in $d = 2$. Nonlinearities can be analyzed by a dynamical renormalization group (DRG) [21] approach. In this procedure, one first averages the slow fields nonlinear equations of motion over the short-wavelength fluctuations and then, in order to restore the ultraviolet cut-off of the theory, rescales length-scales, timescales and the slow fields [2] according to $r_{\perp} = br'_{\perp}$, $r_{\parallel} = b^{\xi}r'_{\parallel}$ $t = b^z t'$, $v_{\perp} = b^{\chi}v'_{\perp}$ and $\delta\rho = b^{\chi}\delta\rho'$. Here $b > 1$ is the (arbitrary) rescaling factor involved in both the averaging and rescaling steps and the scaling exponents χ, ξ e z are known as the 'roughness', 'anisotropy' and 'dynamical' exponents. By this procedure one obtains increasingly coarse-grained hydrodynamic equations with new coefficients $\mu^{(b)}$. By a proper choice of the scaling exponent, the DRG flow typically converges to a nonlinear fixed point (FP) μ^* that captures the long-wavelength behavior of the theory. It can be shown that at this nonlinear fixed point the structure factors S_{ρ} and S_v share the same scaling in the transversal direction, that is for $q_{\perp}^{\xi} \gg q_{\parallel}$,

$$S_v(q_{\perp},q_{\parallel},\boldsymbol{\mu}^*) \sim S_{\rho}(q_{\perp},q_{\parallel},\boldsymbol{\mu}^*) \sim q_{\perp}^{-\zeta}\,. \tag{7}$$

[1] The pedex "0" denotes that the coefficients are evaluated for $\rho = \rho_0$ and $|\mathbf{v}| = v_0$.

[2] One may show that transversal velocity and density fluctuations have the same scaling [10].

where $\zeta \equiv d-1+\xi+2\chi$. Note that correlations may only depend on the modulo of the wavenumber in the symmetry unbroken transversal directions.

In the longitudinal direction, $q_\parallel \gg q_\perp^\xi$, transversal velocity correlations scale as

$$S_v(q_\perp, q_\parallel, \boldsymbol{\mu}^*) \sim q_\parallel^{-\zeta/\xi}\,. \tag{8}$$

while the situation is less clear for the density structure factor. TT theory predicts

$$S_\rho(q_\perp, q_\parallel, \boldsymbol{\mu}^*) \sim q_\perp^2 q_\parallel^{-2-\zeta/\xi}\,. \tag{9}$$

while numerical simulations suggest a different and more complex behavior[14], which will be briefly discussed in Sec. II C. This discrepancy, still poorly understood, is probably due to the singular behavior of the linear density structure factor for $q_\perp \to 0$ discussed above.

The exact value of the nonlinear FP scaling exponent for $d < d_c$ has long remained elusive due to the pletora of potentially relevant nonlinear terms in the TT equations. Recent analytical developments, however, suggest that in the DRG procedure the noise vertex should not acquire graphical corrections due to the (previously overlooked) gradient structure of the symmetry broken theory and that a further generalized Galilean invariance of the theory preserves other nonlinear coefficients at least for $d = 2$. A straightforward calculation leads to the $d = 2$ scaling exponents [16]

$$\chi = -1/3 \quad , \quad \xi = 1 \quad , \quad z = \zeta = 4/3 \tag{10}$$

in agreement with large scale simulations results for the Vicsek model[14]. While $\xi = 1$ implies, at least in $d = 2$, no spatial anisotropy between the longitudinal and transversal directions[3], in the following we derive our result for the general case $\xi \leq 1$.

B. Scaling of transversally confined flocks

In the presence of transversal confinement by reflecting or partially reflecting walls, the average direction of collective motion aligns along the channel. The scaling behavior of the structure factors can then be deduced by a finite size scaling analysis and the request that for a diverging confinement length $L_\perp \to \infty$ one should recover the scaling results of bulk Toner & Tu theory.

[3] A different approach [22], based on the nonperturbative functional renormalization group, suggests a slightly different set of scaling exponent, in particular $\xi = 0.955$ for $d = 2$. While the difference with the exponents put forward in Refs. [15, 16] is so small to be beyond the precision of current numerical estimates, it should be remarked that the results of [22] rely on a number of uncontrolled approximations.

Taking into account the dependence on $L_\perp$, the structure factors S_ρ and S_v, here collectively denoted as S, obey the following DRG scaling law

$$S(q_\perp, q_\parallel, \boldsymbol{\mu}^{(1)}, L_\perp^{-1}) = b^\zeta S(bq_\perp, b^\xi q_\parallel, \boldsymbol{\mu}^{(b)}, bL_\perp^{-1}) \tag{11}$$

where the scaling of the structure factors has been determined considering that they are given by the Fourier transform of the equal time, real space density correlation function. Thus, it involves two powers of the density fluctuations and one volume element, leading to the scaling exponent $d-1+\xi+2\chi = \zeta$.

We choose $bL_\perp^{-1} = 1$ which implies $b = L_\perp$. For a sufficiently large separation, $L_\perp \gg 1$, we have $\boldsymbol{\mu}^{(b)} \simeq \boldsymbol{\mu}^*$ and we obtain

$$S(q_\perp, q_\parallel, \boldsymbol{\mu}^{(1)}, L_\perp^{-1}) = L_\perp^\zeta S(L_\perp q_\perp, L_\perp^\xi q_\parallel, \boldsymbol{\mu}^*, 1) \tag{12}$$

where

$$S(x, y, \boldsymbol{\mu}^*, 1) \equiv g(x, y) \tag{13}$$

is a universal scaling function. We analyze two different regimes, depending on whether the behavior of S is dominated by the longitudinal or transverse wave numbers.

When $q_\perp^\xi \gg q_\parallel$, in the long wavelength limit we consider the one parameter universal scaling function $w_\perp(x) \equiv g(x, 0) = S(x, 0, \boldsymbol{\mu}^*, 1)$ which yields the scaling

$$S(\mathbf{q}, L_\perp^{-1}) = L_\perp^\zeta w_\perp(L_\perp q_\perp) \tag{14}$$

The behavior of the universal scaling function $w_\perp$ can be inferred by the request that, for $L_\perp \to \infty$, the structure factor scaling coincides with the one of Eq. (7) and that a tight confinement $L_\perp \to 0$ suppresses the scale free divergence at small wave-numbers preserving a finite variance,

$$w_\perp(x) \sim \begin{cases} x^{-\zeta} & x \gg 1 \\ \text{constant} & x \ll 1 \end{cases} \tag{15}$$

The simplest expression for the scaling function is thus

$$w_\perp(L_\perp q_\perp) \sim \frac{1}{(L_\perp q_\perp)^\zeta + G_\perp}, \tag{16}$$

where $G_\perp$ is a phenomenological parameter depending (among other things) on microscopic boundary conditions. Then, for sufficiently small wavenumbers, the structure factors S_ρ and S_v take the form

$$\begin{aligned} S_\rho(\mathbf{q}, L_\perp^{-1}) &\sim \frac{L_\perp^\zeta}{(L_\perp q_\perp)^\zeta + G_\perp^{(\rho)}} = \frac{1}{q_\perp^\zeta + G_\perp^{(\rho)} L_\perp^{-\zeta}} \\ S_v(\mathbf{q}, L_\perp^{-1}) &\sim \frac{L_\perp^\zeta}{(L_\perp q_\perp)^\zeta + G_\perp^{(v)}} = \frac{1}{q_\perp^\zeta + G_\perp^{(v)} L_\perp^{-\zeta}} \end{aligned} \tag{17}$$

for $q_\perp^\xi \gg q_\parallel$ and with possibly different phenomenological parameters $G_\perp^{(\rho)}$ and $G_\perp^{(v)}$.

An analogous derivation for the transversal velocity correlation in the longitudinal case, $q_\perp^\xi \ll q_\parallel$, introduces the longitudinal scaling function $w_\parallel(y) \equiv g(0,y) = S_v(0,y,\boldsymbol{\mu}^*,1)$, whose behavior is also determined by matching with Eq. (8) for $L_\perp \to \infty$,

$$w_\parallel(L_\perp q_\parallel) \sim \frac{1}{(L_\perp^\xi q_\parallel)^{\zeta/\xi} + G_\parallel}, \tag{18}$$

with the phenomenological parameter $G_\parallel$ also depending on boundary conditions. It follows that when $q_\parallel \gg q_\perp^\xi$ the structure factor for the transversal velocity takes the form

$$S_v(\mathbf{q}, L_\perp^{-1}) \sim \frac{L_\perp^\zeta}{(L_\perp^\xi q_\parallel)^{\zeta/\xi} + G_\parallel} = \frac{1}{q_\parallel^{\zeta/\xi} + G_\parallel L_\perp^{-\zeta}} \tag{19}$$

The density structure factor in the longitudinal direction, on the other hand, presents an anomalous scaling which will be discussed at the end of this section.

Eqs. (17) and (19) express the scaling of the density and transversal velocity static correlations in Fourier space for transversally confined flocking. They show how confinement induces an effective mass term $M_c \sim L_\perp^{-\zeta}$ nominally suppressing the bulk fluctuations divergence at small wave-numbers. Transversal confinement, however, implies that $q_\perp$ is a positive integer multiple of $\pi/L_\perp$. The mass corrections is only relevant for transversal wave-numbers such that $(L_\perp q_\perp)^\zeta \lesssim G_\perp$, which implies

$$G_\perp \gtrsim \pi^\zeta \,. \tag{20}$$

We conclude that for $G_\perp$ of order one or smaller the suppression of the divergence may well not be detectable along the confined directions.

This is not the case in the longitudinal direction. For an infinite system, $q_\parallel$ is unbounded from zero and a plateau in the transversal velocity structure factor should appear for $q_\parallel \lesssim G_\parallel^{\xi/\zeta} L_\perp^{-\xi}$. In numerical or experimental systems one typically deals with periodic boundary conditions in the longitudinal direction (i.e. a ring geometry) and a longitudinal size $L_\parallel$ with a corresponding smallest longitudinal wavenumber $\pi/L_\parallel$. Boundary effects thus generate a detectable suppression of the small wavelength divergence for

$$G_\parallel \gtrsim \left(\frac{L_\perp^\xi}{L_\parallel}\pi\right)^{\zeta/\xi} . \tag{21}$$

We finally discuss the density structure factor scaling for $q_\perp^\xi \ll q_\parallel$. The lack of a clear analytical understanding of the free theory behavior of S_ρ in the longitudinal direction prevents us from formulating a precise scaling form for confined systems, but nevertheless we still expect that the explicit symmetry breaking will result in

$$S_\rho(0, q_\parallel, L_\perp^{-1}) \xrightarrow{q_\parallel \to 0} \frac{1}{\Sigma(L_\perp)} \tag{22}$$

with $\Sigma(L_\perp)$ an anomalous mass term scaling with a negative power of $L_\perp$.

We have derived the scaling of velocity correlations in the transversal and longitudinal directions, even if, as previously discussed, recent results predict no scaling anisotropy ($\xi = 1$) in Vicsek flocks. However, this scaling isotropy does not imply that also the prefactors have to be equal, leading to the general scaling form

$$S_v(\mathbf{q}, L_\perp^{-1}) \sim \frac{1}{q^\zeta + G(\theta_\mathbf{q}) L_\perp^{-\zeta}} \tag{23}$$

where $G(\theta_\mathbf{q})$ is phenomenological parameter with $G(0) = G_\parallel$ and $G(\pi/2) = G_\perp^{(v)}$.

Note finally that these results have been derived without any explicit modelling of the interaction between the active particles and the confining walls. The only requirement is that the rotational invariance of the self-propulsion orientation is explicitly broken at the boundaries. This clearly applies to reflecting or partially reflecting boundaries, or more generally to any systems in which the proximity with the wall induces – directly or indirectly - torques on the self-propulsion orientation, thus avoiding the trapping of active particles by the wall.

C. Numerical evidence

These predictions can be verified considering the Vicsek model (VM) [23, 24] – the prototypical microscopic flocking model – transversally confined by reflecting boundary conditions. In two spatial dimensions, the discrete time dynamics of N active particles with position $\mathbf{r}_i^t$ and unit self-propulsion orientation $\mathbf{s}_i^t = (\cos\theta_i^t, \sin\theta_i^t)$ is given by

$$\theta_i^{t+1} = \mathrm{Arg}\left(\sum_{j\sim i} \vec{s_j}^t\right) + \eta\xi_i^t, \quad \vec{r_i}^{t+1} = \vec{r_i}^t + v_0 \vec{s_i}^{t+1}, \tag{24}$$

where $j \sim i$ indicates that the corresponding sum is carried over all the particles j within unit distance of i (including i itself) and $\mathrm{Arg}(\vec{u})$ returns the angle defining the orientation of $\vec{u}$. The active particles move with constant speed v_0 and their orientation is subject to a zero-average and delta-correlated scalar noise term of amplitude η, with the ξ_i^t being independent variables uniformly drawn from the interval $[-\pi, \pi]$. We consider periodic boundary conditions in the longitudinal direction of size $L_\parallel$ and implement the transversal reflecting boundaries by the following collision rule [25]

$$s_\perp \to -s_\perp \quad , \quad r_\perp \to 2B - r_\perp \tag{25}$$

with either $B = 0$ (left boundary) or $B = L_\perp$ (right boundary), which is applied whenever the Vicsek dynamics (24) would result in a particle position with transversal component $r_\perp$, outside the region $r_\perp \in [0, L_\perp]$.

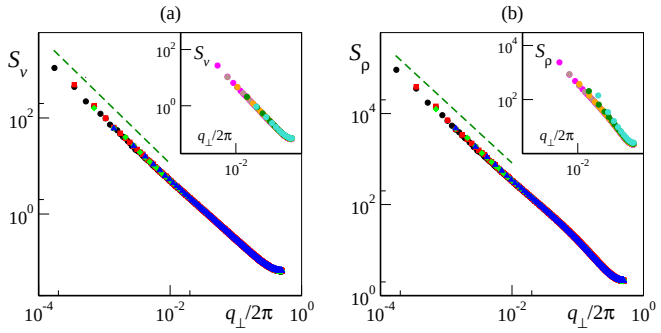

FIG. 1: **Equal time Fourier correlations in the transverse direction.** (a) Transversal velocity correlations and (b) Density fluctuation correlations. Transversal system sizes are $L_\perp = 8192$ (black circles), $L_\perp = 4096$ (red squares), $L_\perp = 2048$ (green diamonds), $L_\perp = 1024$ (blue traingles). The dashed green line marks a power law divergence with exponent $\zeta = 1+\xi+2\chi = 4/3$ [14, 16]. Correlations for smaller transversal separations, $L_\perp = 32, 64, 128, 256, 512$, are shown in the two insets.

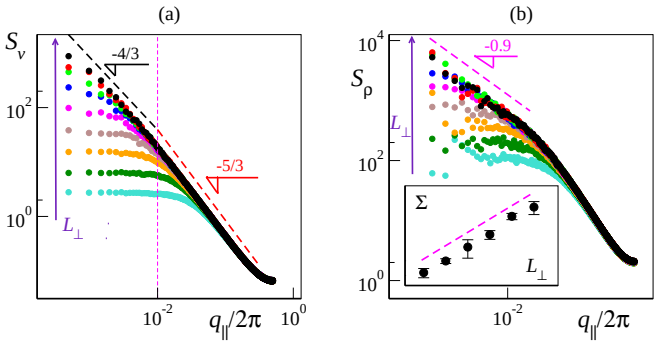

FIG. 2: **Equal time Fourier correlations in the longitudinal direction.** (a) Transversal velocity correlations. The vertical dashed line marks the crossover scale $q_c/(2\pi) = 10^{-2}$ separating the asymptotic regime (dashed black line with scaling exponent 4/3) from the finite size one (dashed red line with scaling exponent $\approx 5/3$) (see text). (b) Density fluctuation correlations. In both panels transversal separations are, from bottom to top, $L_\perp = 32, 64, 128, 256, 512, 1024, 2048, 4096, 8192$. The dashed magenta line marks an algebraic divergence with an exponent 0.9. Inset: Scaling of the effective mass term Σ as a function of transversal separation. The dashed magenta line marks an algebraic growth with an exponent 0.9.

In the following, we place ourselves in the polar liquid phase of the non-confined model [26, 27] by fixing $v_0 = 0.5$, $\eta = 0.2$ and $\rho_0 = N/(L_\parallel L_\perp) = 2$ and we consider more than two orders of magnitude range of values for the transverse separation distance, from $L_\perp = 32$ to $L_\perp = 8192$, keeping the longitudinal size constant, $L_\parallel = 2048$. For numerical convenience, we mainly consider uniform initial positions with alignment parallel to the confining walls, but we have also verified that also different initial conditions always lead, after a transient, to a polar state with the mean flocking direction typically aligned along the longitudinal direction.

In order to measure the density and transversal velocities structure factors, we first obtain fluctuating fields for the density $\delta\rho(\mathbf{r})$ and the perpendicular velocity $v_\perp(\mathbf{r})$ by coarse-graining the microscopic particles number and transversal velocities over boxes of unit linear length. In order to avoid densities inhomogeneities near the confining walls [25] we only evaluate the fields in a central channel of extension $0.7L_\perp$, thus excluding two regions of size $0.15L_\perp$ adjacent to the walls. The resulting Fourier space static correlations

$$S_\rho(\mathbf{q}) \equiv \langle|\delta\hat{\rho}(\mathbf{q})|^2\rangle \quad , \quad S_v(\mathbf{q}) \equiv \langle|\hat{v}_\perp(\mathbf{q})|^2\rangle \tag{26}$$

are also averaged in time (after a proper transient has been discarded) over typically 10^6 timesteps.

We first fix $q_\parallel = 0$ in order to probe correlations in the transversal direction. Their behavior, reported in Fig. 1, does not show any sign of suppression of the small $q_\perp$ divergence which, for sufficiently large separations $L_\perp$, shows an excellent agreement with the predicted $d = 2$ bulk exponent $\zeta = 1 + \xi + 2\chi = 4/3$ [15, 16]. This implies that, at least for typical Vicsek dynamics transversally confined by reflecting walls, condition (20) on the phenomenological parameters $G_\perp^{(\rho)}$ and $G_\perp^{(v)}$ is not met.

The behavior of velocity correlations in the longitudinal direction (see Fig. 2a), obtained by setting $q_\perp = 0$, is different, with a clear suppression of the low $q_\parallel$ divergence for small transversal separations $L_\perp \lesssim L_\parallel$, where condition (21) is met. Only when $L_\perp \gtrsim L_\parallel$ one cannot clearly identify a plateau for small $q_\parallel$, and the structure factor approaches the free theory algebraic divergence (19).

We have also tested the density structure factor in the longitudinal direction fixing($q_\perp = 0$), results shown in Fig. 2b. Also in this case, a plateau for $q_\parallel \ll 1$ is evident for $L_\perp \lesssim L_\parallel$. At larger longitudinal wavenumber, an anomalous slow scaling behavior $\sim q_\perp^{-\gamma}$, first reported in [14], becomes apparent [4], although our numerical estimates suggest a slightly larger exponent, $\gamma \approx 0.9$. Applying the scaling arguments developed in Sec. II B to this empirical scaling behavior immediately gives the scaling

$$S_\rho(0, q_\parallel, L_\perp^{-1}) \sim \frac{1}{q_\parallel^\gamma + \Sigma(L_\perp)} \tag{27}$$

with the anomalous effective mass term scaling

$$\Sigma(L_\perp) \sim L_\perp^{-\gamma} . \tag{28}$$

When $L_\perp \lesssim L_\parallel$ is possible to measure Σ by evaluating $S_\rho(0, q_\parallel, L_\perp^{-1})$ in the limit $q_\parallel \to 0$. Our results, shown

[4] In Ref. [14] it was also reported an intermediate scaling regime, in qualitative agreement with Eq. (9) which, however, should be unobservable for $q_\perp \to 0$.

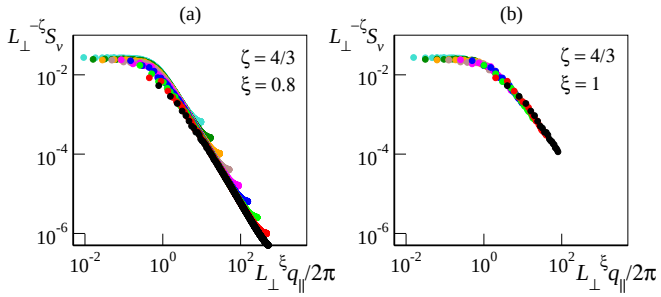

FIG. 3: **Velocity structure factor data collapses in the longitudinal direction.** (a) Structure factor data from Fig. 2 rescaled according to Eq. (29) with scaling exponents $\zeta = 4/3$ and $\xi = 0.8$. (b) Same data, but only for $q_\parallel < q_c$ (see text) rescaled with scaling exponents $\zeta = 4/3$ and $\xi = 1$. Color coding for different $L_\perp$ as in Fig. 2a.

in the inset of Fig. 2b confirm the scaling (28) with $\gamma \approx 0.9$.

The scaling behavior predicted by Eq. (19) also implies that the velocity structure factor S_v measured for different transversal separation $L_\perp$ should collapse to a universal curve $f(x)$ when properly rescaled,

$$L_\perp^{-\zeta} S_v(0, L_\perp^{\xi} q_\parallel) \equiv f(x)\,. \tag{29}$$

When testing this result by data-collapse, however, one should be aware that the most accurate numerical simulations of longitudinal structure factors (see Ref. [14]) revealed large finite size effects. In particular in $d = 2$ the anisotropy exponent ξ shows a crossover behavior from a finite-size (for $q > q_c$) value $\xi \approx 0.8$ to the asymptotic (for $q < q_c$) one $\xi = 1$ as also shown in Fig. 2a where the power law scaling crosses over from an exponent $\zeta/\xi = 5/3$ to $\zeta/\xi = 4/3$. For Vicsek dynamics with scalar noise it was found $q_c/(2\pi) \approx 10^{-2}$, as marked in Fig. 2 by the vertical dashed lines. Transversal correlations, on the other hand, do not show such crossover and one can confidently use $\zeta = 4/3$ over a wider range of scales.

In Fig. 3a we first attempt to rescale the data of Fig. 2a by using the pre-crossover scaling exponents $\zeta = 4/3$ and $\xi = 0.8$. While one may observe a reasonable collapse at large enough $q_\parallel$ values, a closer inspection reveals a less satisfactory collapse at smaller wave-numbers. The small $q_\parallel$ collapse may be improved rescaling the data with the post crossover value $\xi = 1$, as shown in Fig. 3b where only the data for $q_\parallel < q_c$ is considered.

To summarise, numerical simulations of Vicsek dynamics in the confined polar liquid phase confirm that bulk correlations in the transversal direction are not affected by the reflecting boundaries. In the longitudinal direction, our numerics support the scaling form (19) for the transversal velocity structure factor and suggest the empirical anomalous effective mass term (28) for density correlations.

III. ORDER PARAMETER BEHAVIOR AND EQUIVALENCE WITH DRIVEN SYSTEMS

A. Longitudinal response

We now turn our attention to the behavior of the order parameter in the presence of transversal confinement. Microscopically, the instantaneous global order parameter is defined as

$$\Omega(t) = \frac{1}{N}\sum_{i=1}^{N} \mathbf{s}_i^t\,. \tag{30}$$

The scalar order parameter is given by $\Phi = \langle|\Omega(t)|\rangle_t$, where $\langle\cdot\rangle$ denotes temporal averages. Here we are interested in the static longitudinal response, that is, the difference in the scalar order parameter between the confined and the bulk system,

$$\delta\Phi(L_\perp) = \Phi(L_\perp) - \Phi(\infty) \tag{31}$$

At the hydrodynamic level, the scalar order parameter can be obtained by the spatial and temporal average of Eq. (4). Since linear terms in $\delta\rho$ and $\mathbf{v}_\perp$ all vanish under such averages, one is left with

$$\Phi = p_0 + \langle \delta v_\parallel \rangle \approx p_0 - \frac{\langle|\mathbf{v}_\perp|^2\rangle}{2p_0}\,, \tag{32}$$

the analogous of the so-called principle of conservation of the modulus that links longitudinal and transversal fluctuations in equilibrium ferromagnets [28].

From Eq. (31) it follows that the order parameter response is thus given by

$$\begin{aligned}\delta\Phi(L_\perp) &= \frac{1}{2p_0}\left[\langle|\mathbf{v}_\perp(\infty)|^2\rangle - \langle|\mathbf{v}_\perp(L_\perp)|^2\rangle\right] \\ &= \frac{1}{2p_0} C_v(0, L_\perp^{-1}, \boldsymbol{\mu}^{(1)})\end{aligned} \tag{33}$$

where we have recognized the real space correlation function

$$C_v(0, L_\perp^{-1}, \boldsymbol{\mu}^{(1)}) = \langle|\mathbf{v}_\perp(\infty)|^2\rangle - \langle|\mathbf{v}_\perp(L_\perp)|^2\rangle \tag{34}$$

and assumed $L_\parallel \to \infty$. We can deduce the scaling behavior of the response $\delta\Phi$ by repeating in real space essentially the same finite size scaling analysis performed in section II B. Performing a DRG step with a rescaling factor b one obtains

$$C_v(0, L_\perp^{-1}, \boldsymbol{\mu}^{(1)}) = b^{2\chi} C_v(0, bL_\perp^{-1}, \boldsymbol{\mu}^{(b)}) \tag{35}$$

where the scaling of the correlation function is determined by the fact that it just involves a squared field. Choosing as before $b = L_\perp$ we finally obtain, for a sufficiently large spatial separation $L_\perp \gg 1$,

$$C_v(0, L_\perp^{-1}, \boldsymbol{\mu}^{(1)}) = L_\perp^{2\chi} C_v(0, 1, \boldsymbol{\mu}^{*}) \tag{36}$$

with the r.h.s. parameters now evaluated at the nonlinear fixed point. Eq.(36) immediately implies the response scaling

$$\delta\Phi(L_\perp) \sim L_\perp^{2\chi} . \tag{37}$$

This asymptotic scaling can be verified by microscopic simulations of the Vicsek dynamics. Fig. 4a shows the convergence of the scalar order parameter to its asymptotic value fixed by p_0. In order to estimate the convergence to this asymptotic value we consider the centered finite difference $\partial_c\Phi(L_\perp)$ of the average order parameter, which approximates the first derivative of $\Phi(L_\perp)$ up to corrections of third order in the derivatives. We can then estimate the response as

$$\delta\Phi \sim L_\perp \partial_c \Phi(L_\perp) . \tag{38}$$

From Fig. 4b we can see that its asymptotic behavior well matches our prediction, while a crossover is observed for smaller transversal separation sizes. This should not come as a surprise: we have seen in Sec. II C that in $d = 2$ the anisotropy exponent ξ shows a finite size crossover from ≈ 0.8 to its asymptotic value $\xi = 1$. Since $\zeta = d-1+\xi+2\chi = 4/3$ remains constant over a wider range of scales, this implies that also the roughness exponent should cross-over from the finite size value $\chi \approx -0.2$ to its asymptotic value $\chi = -1/3$.

B. Equivalence with homogeneously driven systems and fluctuations in the mean flocking direction

It is instructive to compare these results with the behavior of flocking systems in the presence of a homogeneous external field $\mathbf{h}$ of amplitude $h = |\mathbf{h}|$ driving each active particle orientation. Ref. [17] it was shown that in the linear regime (valid for small field amplitudes) and large system sizes, the response scales as

$$\delta\Phi(h) \equiv \Phi(h) - \Phi(0) \sim h^{-2\chi/z} . \tag{39}$$

Similarly, it is known from Ref. [18] that an external homogeneous field breaks explicitely the rotational symmetry and thus induces an effective mass term $\sim h^{\zeta/z}$ or, thanks to the hyperscaling relation $\zeta = z$, see Eq. (10), more simply $\sim h$. The structure factors thus read

$$S(\mathbf{q}, h) \sim \frac{1}{q_\perp^\zeta + D_\perp h^{\zeta/z}} , \tag{40}$$

in the direction transversal w.r.t. to the external field and

$$S(\mathbf{q}, h) \sim \frac{1}{q_\parallel^{\zeta/\xi} + D_\parallel h^{\zeta/z}} \tag{41}$$

in the direction parallel to $\mathbf{h}$ (once again, these two scalings coincide for $\xi = 1$).

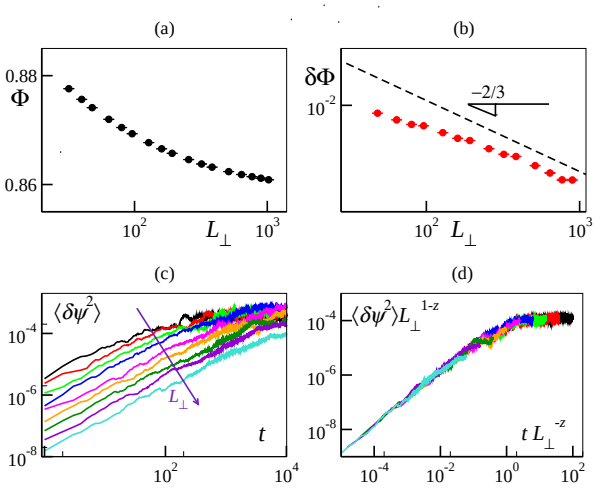

FIG. 4: **Order parameter scaling.** (a) Scalar order parameter Φ as a function of the transversal separation size. (b) Order parameter static response $\delta\Phi$, as a function of the transversal separation size, evaluated from panel (a) by Eq. (38). System parameters are $L_\parallel = 512$, $\rho_0 = 2$, $v_0 = 0.5$ and $\eta = 0.21$. Data has ben averaged over around 10^5 *independent* datapoints. Error bars mark two standard errors. The dashed line marks the expected asymptotic power law decay with an exponent $2\chi = -2/3$. (c) Mean squared fluctuations in the flocking direction for increasing transversal separation sizes, from top to bottom $L_\perp = 32, 64, 128, 256, 512, 1024, 2048, 4096, 8192$. (d) Data collapse of the data in panel (c) according to Eq. (47) with dynamical scaling exponent $z = 4/3$. Data in panels (c)-(d) has been averaged over 10^2 different realizations with parameters $L_\parallel = 2048$, $\rho_0 = 2$, $v_0 = 0.5$ and $\eta = 0.2$.

Comparison between the response scalings (37)-(39) and the structure factors (17)-(40) and (19)-(41) immediately suggests the equivalence between trasversal confinement by reflecting boundaries, a local form of explicit symmetry breaking, and the presence of a homogeneous external driving field (which explicitly breaks the rotational symmetry at bulk level) of amplitude [5]

$$h \sim L_\perp^{-z} . \tag{42}$$

We test this equivalence on the fluctuations of the fluctuations of the mean flocking direction $\psi(t) = \mathrm{Arg}[\Omega(t)]$. In Ref. [18], it has been shown by mean-field like approximations of the microscopic VM dynamics, that $\psi(t)$ obeys an Ornstein-Uhlenbeck process. In particular, we are interested in the fluctuations of the mean flocking direction, $\delta\psi(t) = \psi(t) - \psi(0)$ with the initial condition $\psi(0)$ aligned in the external field direction. The mean

[5] Note that this relation holds on dimensional grounds since the field amplitude scales as the inverse of a time [17].

squared fluctuations are thus given by

$$\langle \delta\psi(t)^2 \rangle \approx \frac{D_\psi}{h'} \left(1 - e^{-2h't}\right) \tag{43}$$

where $h' = h/\bar{m}$, with $\bar{m}$ being the average number of interacting particles in the Vicsek dynamics (24), plays the role of the confining potential stiffness [6] and

$$D_\psi = \frac{\eta^2 \pi^2}{6N} \tag{44}$$

is (twice) the effective diffusion acting on the mean flocking orientation. Eq. (43) implies that $\langle \delta\psi^2 \rangle$ will grow linearly as $2D_\psi t$ on short timescales, $t \ll 1/(2h')$, eventually saturating to a constant value D_ψ/h' for $t \gg 1/(2h')$. In practice, the short time dynamics of $\psi(t)$ is diffusive and cannot be distinguished from the zero field behavior, while at large enough time the external field suppresses orientation diffusion and acts as a confining potential on the mean flocking direction.

We now consider fluctuations of the mean flocking directions in the absence of an external field but for a transversally confined flock. Carrying on the correspondence expressed by Eq. (42) and using $N = \rho_0 L_\parallel L_\perp$ one gets by direct substitution in Eq. (43)

$$\langle \delta\psi(t)^2 \rangle = \frac{\eta^2 \pi^2}{6\rho_0 L_\perp L_\parallel} \frac{\bar{m}}{L_\perp^{-z}} \left[1 - \exp\left(-\frac{2L_\perp^{-z}}{\bar{m}} t\right)\right] \tag{45}$$

or, introducing the scaling function

$$f(x) \equiv \frac{\eta^2 \pi^2 \bar{m}}{6\rho_0 L_\parallel} \left[1 - \exp\left(-\frac{2}{\bar{m}} x\right)\right], \tag{46}$$

$$\langle \delta\psi(t)^2 \rangle = L_\perp^{z-1} f(L_\perp^{-z}\, t)\,. \tag{47}$$

Transversal confinement between parallel reflecting walls thus suppresses diffusion of the mean flocking directions at large enough times, with

$$\langle \delta\psi(\infty)^2 \rangle \sim L_\perp^{z-1} \tag{48}$$

while at short times ($t \ll L_\perp^z \bar{m}/2$) one has a diffusive behavior with

$$\langle \delta\psi(t)^2 \rangle \approx \frac{\eta^2 \pi^2}{3\rho_0 L_\parallel L_\perp}\, t\,. \tag{49}$$

Microscopic numerical simulations, reported in Fig. 4c, clearly show these two regimes. In particular, data collapse (see Fig. 4d) confirms the scaling form (47), thus supporting the equivalence conjectured in (42).

[6] Note that this potential confines the mean flocking orientation, not the position of the active particles.

IV. DISCUSSION

In this work, we have shown by analytical and numerical arguments that transversal confinement between parallel reflecting walls separated by a distance $L_\perp$ introduces an effective mass term $M_c \sim L_\perp^{-\zeta}$ damping the free theory Nambu-Goldstone mode.

The effect of confinement on bulk connected correlations can be deduced by standard finite size scaling analysis under the rather generic assumption that the transversal boundaries break the rotational symmetry of the active particles self propulsion orientation. In principle the mass term should suppress the small wavenumber divergence of fluctuations correlations in Fourier space (or, equivalently, introduces an exponential cut-off in the real space connected correlations), introducing a crossover towards a finite value,

$$S(\mathbf{q} \to 0) \sim M_c^{-1}\,. \tag{50}$$

This crossover is however controlled by phenomenological constants which in principle depends on microscopic parameters and on the details of the interaction with the confining boundaries. In the transversal direction, where wave-numbers are bounded from below due to the finiteness of the sytem, this implies that the saturation regime does not appear for a phenomenological constants $G_\perp$ of order one or smaller. We have verified numerically that this is for instance the case for the standard VM model confined between parallel reflecting walls.
In the longitudinal direction, on the other hand, such a crossover can be observed in a narrow enough ring configuration, that is for $L_\perp \lesssim L_\parallel$. Density correlation in the longitudinal direction, however, seem to be characterized by an anomalous effective mass term $\Sigma \sim L_\perp^{-\gamma}$, with $\gamma \approx 0.9$ an empirical scaling factor of unknown origin.

Confinement also increases the scalar order parameter values, which shows an algebraic decay to its asymptotic value with increasing separation sizes,

$$\Phi(L_\perp) - \Phi(L_\perp \to \infty) \sim L_\perp^{2\chi}\,. \tag{51}$$

Since this result has been obtained only by finite scaling analysis, it does not depend in any way on the nature of boundary conditions, and should also apply to the standard numerical setup of finite systems with periodic boundary conditions (PBC), as it has been already realized in [29]. Indeed, numerical simulation of the VM in two dimensional tori of linear size L show a power law decay of the scalar order parameter to its asymptotic value, $\Phi(L) - \Phi(L \to \infty) \sim L^\alpha$, with an exponent $\alpha \approx -0.64$ [2] compatible with the theoretical prediction $\alpha = 2\chi = -2/3$. Interestingly, this result suggest an alternative and more robust way to estimate numerically the theory scaling exponent from the finite size scaling of global observables rather than from the measure of the small wavelength behavior of correlation functions.

Altogether, these results suggest an equivalence between the effects of an explicit symmetry breaking due to boundary conditions and the one induced by an homogeneous (and small) external driving of amplitude h. Both induce an effective mass term, with the equivalence $M_c \sim h \sim L_\perp^{-z}$. This mass term, finally, constrains the mean flocking direction $\psi(t)$ fluctuations acting as an effective harmonic potential stiffness which, at large times, prevents the diffusion of $\psi(t)$ that characterize free finite flocks.

We believe our results could be of experimental relevance and can be tested by confining flocking systems such as active colloids [6] or flocking epithelial tissues [4]. In the future it could be interesting to extend our result to the case of flocking at a solid-liquid interface discussed in [30].

Acknowledgments

We thank B. Mahault for valuable discussions. We acknowledge support from PRIN 2020PFCXPEAG.

[1] S. Ramaswamy, Annu. Rev. Condens. Matter Phys. **1**, 323 (2010).
[2] H. Chaté, Annu. Rev. Condens. Matter Phys. **11**, 189 (2020).
[3] M. Ballerini, N. Cabibbo, R. Candelier, A. Cavagna, E. Cisbani, I. Giardina, V. Lecomte, A. Orlandi, G. Parisi, A. Procaccini, et al., Proc. Natl. Acad. Sci. **105**, 1232 (2008).
[4] F. Giavazzi, C. Malinverno, S. Corallino, F. Ginelli, G. Scita, and R. Cerbino, J. Phys. D: Appl. Phys. **50**, 384003 (2017).
[5] V. Schaller, C. Weber, C. Semmrich, E. Frey, and A. R. Bausch, Nature **467**, 73 (2010).
[6] A. Bricard, J. Caussin, N. Desreumaux, D. O., and D. Bartolo, Nature **503**, 95 (2013).
[7] F. Ginelli, Eur. Phys. J. Spec. Top. **225**, 2099 (2016).
[8] N. D. Mermin and H. Wagner, Phys. Rev. Lett. **17**, 1133 (1966).
[9] P. Hohenberg, Phys. Rev. **158**, 383 (1967).
[10] J. Toner and Y. Tu, Phys. Rev. E **58**, 4828 (1998).
[11] A. Cavagna, A. Cimarelli, I. Giardina, G. Parisi, R. Santagati, F. Stefanini, and M. Viale, Proc. Natl. Acad. Sci. **107**, 11865 (2010).
[12] J. Toner and Y. Tu, Phys. Rev. Lett. **75**, 4326 (1995).
[13] J. Toner, Phys. Rev. E **86**, 031918 (2012).
[14] B. Mahault, F. Ginelli, and H. Chaté, Phys. Rev. Lett. **123**, 218001 (2019).
[15] H. Ikeda, arXiv:2403.02086 (2024).
[16] H. Chaté and A. Solon, arXiv:2403.03804 (2024).
[17] N. Kyriakopoulos, F. Ginelli, and J. Toner, New J. Phys. **18**, 073039 (2016).
[18] M. Brambati, G. Fava, and F. Ginelli, Phys. Rev. E **106**, 024608 (2022).
[19] A. Morin and D. Bartolo, Phys. Rev. X **8**, 021037 (2018).
[20] Y. Tu, J. Toner, and M. Ulm, Phys. Rev. Lett. **80**, 4819 (1998).
[21] U. C. Tauber, *Critical Dynamics* (Cambridge University Press, Cambridge, 2014).
[22] P. Jentsch and C. Lee, arXiv:2402.01316 (2024).
[23] T. Vicsek, A. Czirók, E. Ben-Jacob, I. Cohen, and O. Shochet, Phys. Rev. Lett. **75**, 1226 (1995).
[24] G. Grégoire and H. Chaté, Phys. Rev. Lett. **92**, 025702 (2004).
[25] G. Fava, A. Gambassi, and F. Ginelli, arXiv:2211.02644 (2024).
[26] H. Chaté, F. Ginelli, G. Grégoire, and F. Raynaud, Phys. Rev. E **77**, 046113 (2008).
[27] A. P. Solon, H. Chaté, and J. Tailleur, Phys. Rev. Lett. **114**, 068101 (2015).
[28] A. Z. Patashinskii and V. Pokrovskii, Zh. Eksp. Teor. Fiz. **64**, 1445 (1973).
[29] Y. Duan, B. Mahault, Y. Ma, X. Shi, and H. Chaté, Phys. Rev. Lett. **126**, 178001 (2021).
[30] N. Sarkar, A. Basu, and J. Toner, Phys. Rev. Lett. **127**, 268004 (2021).